Journal of Catalysis **184,** 553–556 (1999)
Article ID jcat.1999.2453, available online at http://www.idealibrary.com on

RESEARCH NOTE

Evidence of Furan Formation from Ethanol over β-UO_3

H. Madhavaram and H. Idriss

Materials Chemistry, Department of Chemistry, The University of Auckland, Private Bag 92019, Auckland, New Zealand

Received January 18, 1999; revised February 5, 1999; accepted February 8, 1999

Furan formation during ethanol-TPD over β-UO_3 is observed. Previous work has shown the formation of furan from ethylene-TPD over β-UO_3 (13). The negligible activity of α-U_3O_8 (containing U^{6+} cations representing 86% of total U cations) indicates that the surface structure of β-UO_3 contains the necessary sites. These sites are proposed to be U^{6+} cations with double vacancies to accommodate two ethoxide species followed by coupling to $\overline{CH_2CH_2OU^{6+}OCH_2}CH_2$. Flow experiments of ethanol also indicated the formation of furan, besides acetaldehyde, over β-UO_3 (while α-U_3O_8 was inactive).

Furan and furan derivates are utilised as chemical building blocks in the production of other industrial chemicals for use as pharmaceuticals, herbicides, stabilisers, and fine chemistry (1). Furan is commercially manufactured from the decarbonylation of furfural either by noncatalytic pyrolysis at 700°C (1) or over catalysts based on nickel (2) or cobalt (3). It can also be made by oxidation of butadiene (4, 5). This work presents evidence of furan formation over pure β-UO_3 from ethanol. Over α-U_3O_8 only traces of furan were formed, while UO_2 was inactive. The uranium oxide system, one of the most complex oxides known (6), is one of the richest to investigate. This is due to the wide range of oxidation states of uranium cations (from +2 to +6) and the existence of several stable stoichiometric and super- and substoichiometric bulk structures ranging from UO_{2-x} to UO_3; each of these may present more than one allotropic phase (7). One may divide the observed reactions (catalytic and stoichiometric) of the uranium compounds into two parts: (i) oxidation [such as the ammoxidation of olefins to acrylonitrile on USbO catalysts (8, 9) and the total destruction of chlorinated compounds on U_3O_8 (10)] and (ii) C–C bond formation [such as coupling of ethylene to butadiene on U complexes (11) and reductive coupling of acetaldehyde to butene and butadiene (12) over UO_2]. We have recently successfully combined both routes (oxidation and coupling) into one: oxidative coupling of two molecules of ethylene to furan, C_4H_4O, on polycrystalline β-UO_3 (13). The reaction of acetaldehyde over β-UO_3 is also investigated (12, and work in progress). Although small amounts of furan were observed, the main reaction is that of the β-aldolisation product: crotonaldehyde.

This study was conducted as follows. β-UO_3 was synthesised from uranium nitrate by precipitation with ammonia and calcination at 573 K for 18 h (this method gave us the purest β-UO_3 phase) (14). X-ray diffraction confirmed the absence of any other uranium oxide phase. α-U_3O_8 was obtained from BDH Chemicals, and UO_2 was prepared by H_2 reduction of U_3O_8 (or UO_3) at 1 atm for 12 h (15). X-ray photoelectron spectroscopy (XPS) was previously used to investigate the oxidation states of U cations on the surfaces of UO_2, α-U_3O_8, and UO_3 to quantitatively determine the atomic concentrations of U^{x+} cations on the surface and near surface of these oxides by this group (15). The surface and near surface of the β-UO_3 do not contain U^{4+} cations; i.e., all cations are in a +6 oxidation state. U^{6+} cations in α-U_3O_8 represent ca. 84% of U cations (higher than the theoretical value of 67%, presumably because of surface oxidation of some surface U^{4+} cations), while UO_2 surfaces do not contain any.

A Hiden mass spectrometer (530 amu) in a high vacuum chamber (base pressure ca. 10^{-7} Torr, working pressure during TPD = (2–3) × 10^{-6} Torr) multiplexed to a PC was used to monitor the desorption products during TPD ($\beta = 0.25$ K s^{-1}) at a cyclic rate of ca. 100 amu/10 s. Products were analysed following the method described previously (16). Mass spectrometer correction factors with respect to m/e 28 were calculated following the method described in Ref. (17). The reactor pressure during TPD was ca. 10^{-3} Torr at a pumping speed of ca. 10 m^3/h.

Figure 1 presents TPD after ethanol adsorption over β-UO_3 at room temperature. Unreacted ethanol (m/e 31) desorbs in two temperature domains at 350 and 450 K: both peaks contributed 87% of the overall carbon yield. Acetaldehyde (m/e 29) formed by dehydrogenation of ethanol also desorbed in two temperature domains at 450 and 490 K and contributed 10% of the carbon yield and 77% of the carbon selectivity. Evidence of carbon–carbon bond formation was clear by the desorption of m/e 68 concomitant with

0021-9517/99 $30.00

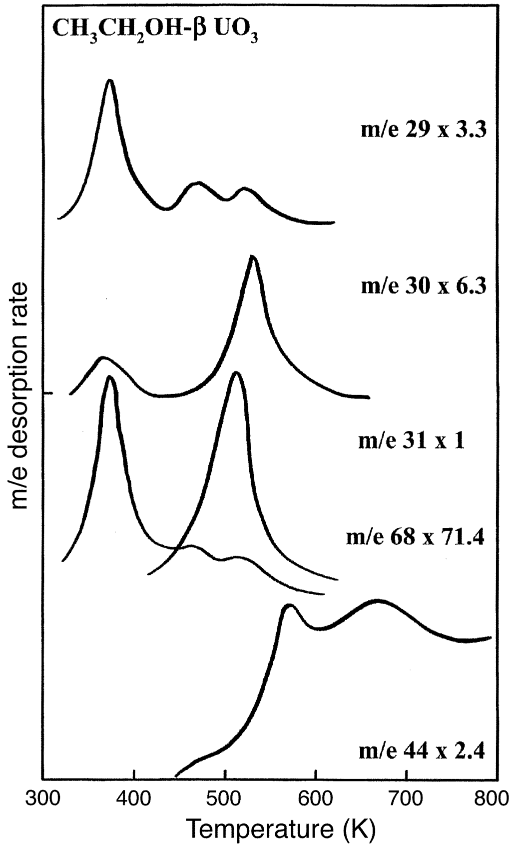

FIG. 1. Product distribution during ethanol-TPD over β-UO_3.

m/e 39 due to furan at 490 K with a carbon yield and carbon selectivity of 3 and 23%, respectively. A peak at m/e 30 was also was observed at 505 K; however, detailed analysis indicated that this peak is a non-carbon-containing molecule and is attributed to NO. Moreover, m/e 44 desorbed in two peaks at 580 and ca. 680 K. The first peak is that of N_2O, while the second is that of CO_2. For quantitative analysis the high-temperature CO_2 desorption is not taken into consideration since it mainly results from bulk carbonate and hydrogenocarbonate decomposition (18). Blank TPD (not shown) showed similar m/e 30 and 44 peak profiles. The carbon yield and carbon selectivities of ethanol/TPD over U_3O_8 were also calculated (Fig. 3) for comparison. The main reaction product is acetaldehyde (98% carbon selectivity) with only traces of furan. UO_2 was inactive for furan formation.

Figure 2 shows ethylene-TPD over β-UO_3. In addition to furan (490 K) both acetaldehyde and ethanol desorbed with a wide peak centered at ca. 500 K. Furan yield is, however, four times lower in the case of ethylene-TDP than in the case of ethanol-TPD. Two major differences exist between the two experiments (Figs. 1 and 2): (1) the absence of ethylene during ethanol-TPD and (2) the formation of both acetaldehyde and ethanol during ethylene-TPD. These indicate that (i) the dehydration route is not favoured over β-UO_3; and (ii) the reaction intermediates for furan formation might be ethoxide species (most likely two vicinal species).

From the above results one may propose the following reaction mechanism. First, coupling of two C2–O species on one uranium cation proceeds as

$$2CH_3CH_2O\ (a) + \mathbf{U}_{6c}^{6+} \rightarrow CH_3CH_2O\mathbf{U}^{6+}OCH_2CH_3. \quad [1]$$

Evidence of coupling reactions over U^+ cations (in the gas phase) has been reported (19), such as ethylene coupling to give $UC_4H_4^+$ and $UC_6H_6^+$. Moreover, a unit lattice of β-UO_3 is composed of five U^{+6} cations: three of them are sixfold-coordinated to oxygen anions (i.e., containing two coordinative unsaturations, U_{6c}^{+6}) and the remaining two are in a pentagonal bypyramid structure (i.e., each U cation is sevenfold-coordinated to oxygen anions) (20). On the other hand, all U cations of α-U_3O_8 are sevenfold-coordinated to oxygen anions, also in a pentagonal bypiramid structure. Thus, it is not surprising that α-U_3O_8 is unreactive for the coupling reaction (the traces observed on α-U_3O_8 might be due to a thin layer of UO_3 formed at the surface of U_3O_8 (not detected by XRD) (see Fig. 3). Second, U catalysts are well known for their dehydrogenation and oxidative

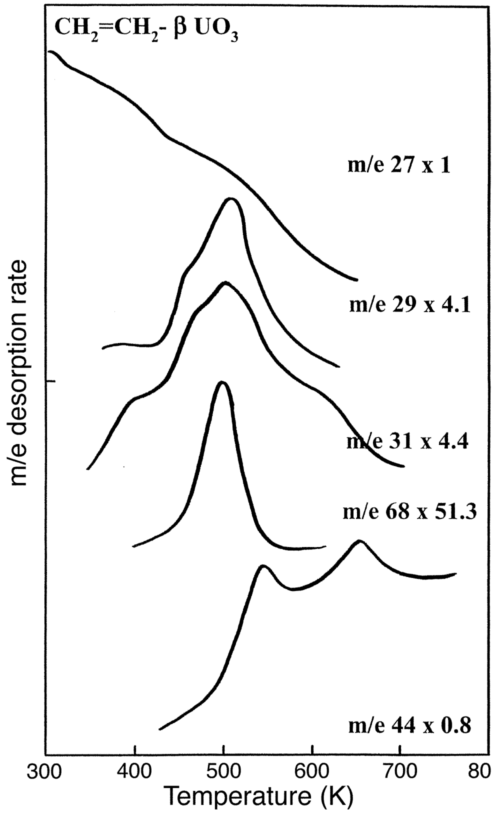

FIG. 2. Product distribution during ethylene-TPD over β-UO_3.

dehydrogenation (8, 9, among others) properties. The abstraction of the β-H atoms followed by the coupling tail to tail of two adjacent species may thus be the limiting step for the reaction

$$CH_3CH_2O\mathbf{U}^{6+}OCH_2CH_3 + 2O^{2-}(l) \rightarrow \overline{CH_2CH_2O\mathbf{U}^{6+}OCH_2}CH_2 + 2OH\ (a) \qquad [2]$$

$$\overline{CH_2CH_2O\mathbf{U}^{6+}OCH_2}CH_2 + 2OH\ (a) + O^{2-}(l) \rightarrow C_4H_4O\ (500\ K) + V_O\mathbf{U}^{x+}O + 3H_2O \qquad [3]$$

$$V_O = \text{oxygen vacancy}, \quad x < 6.$$

The absence of butadience and the presence of ethanol during ethylene-TPD indicates that the above reaction pathway may be very similar, if not the same, for both reactions (ethylene to furan and ethanol to furan). Moreover, the absence of tetrahydrofuran and dihydrofuran during ethylene- and ethanol-TPD indicates that the dehydrogenation route is fast. It is worth indicating that furan desorption is reaction limited since furan desorbed upon room temperature adsorption over β-UO_3 at ca. 350 K.

Preliminary flow experiments using ethanol as a reactant, at atmospheric pressure and temperatures between 423 and 523 K, have shown the following: (1) Ethanol (ca. 2500 ppm) in He indicated initial furan formation (besides acetaldehyde) that decreased with time on stream until disappearance after 3–4 h (acetaldehyde formation was unchanged). (2) The maximum carbon selectivity obtained for furan was 23% with 81% conversion (at $7200\ l\ h^{-1}\ kg^{-1}$, 423 K, and 10^5 Pa) with acetaldehyde as the other product. (3) Substituting He by air resulted in increasing the acetaldehyde selectivity. (4) Increasing the temperature from 423 to 523 K also increased the selectivity to acetaldehyde. (5) XRD after the production of furan stopped indicated partial transformation of β-UO_3 mainly into α-U_3O_8. In effect, thermodynamic limitation requires 3 to 4 MPa of O_2 to revert α-U_3O_8 to β-UO_3 (we have not yet conducted catalytic regeneration at these high pressures). (6) Table 1 shows the total furan production (i.e., the GC furan peak areas have been calculated and integrated as a function of time until no formation is observed) as a function of reaction temperature. Both the amount of furan produced and the fact that this production increased with increasing reaction temperature may indicate that the reaction is not limited to titration of the surface oxygen anions of β-UO_3. (7) furan was not observed over α-U_3O_8.

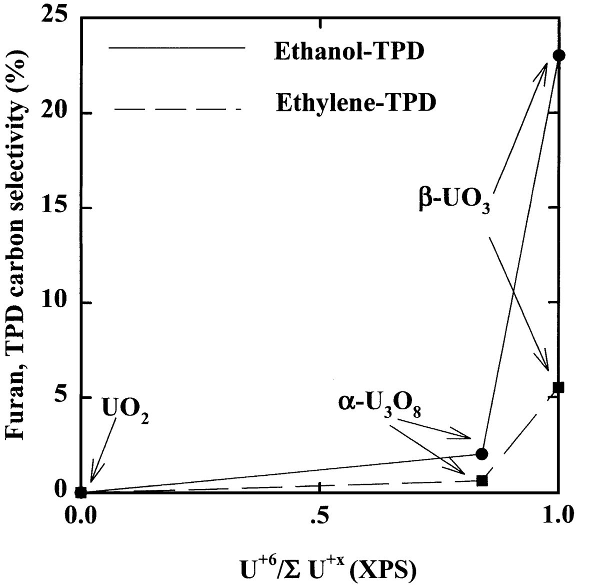

FIG. 3. Furan carbon selectivity (%) versus fraction of U^{6+} cations during ethanol- and ethylene-TPD over β-UO_3, α-U_3O_8, and UO_2; $x = 4, 6$.

TABLE 1

Furan Formation during Flow Experiments of Ethanol/He over β-UO_3[a]

Molecules of furan per g of catalyst	Temperature (K)
2.43×10^{19}	423
6.2×10^{19}	448
1.14×10^{20}	473
1.3×10^{20}	493

[a] BET surface area = 7 m^2/g; F/W = $7200\ l\ h^{-1}\ kg^{-1}$; $T = 423$ K, total pressure = 10^5 Pa, $[\text{Ethanol}]_{in} = (1 \pm 0.1) \times 10^{-7}$ mol/ml.

In summary, this work presents evidence of furan formation over β-UO_3 during ethanol-TPD, ethylene-TPD, and ethanol flow experiments. α-U_3O_8 had negligible activity for this coupling reaction, whereas UO_2 was inactive. As shown in Fig. 3 the change in the U^{6+} population between β-UO_3 and α-U_3O_8 does not explain (by itself) the sharp decrease of the activity. Structural differences are most likely the reason behind the activity difference.

ACKNOWLEDGMENTS

The authors thank the university of Auckland for financial support. This work is dedicated to Professor Warren Roper on the occasion of his 60th birthday.

REFERENCES

1. "Kirk Othmer Encyclopedia of Chemical Technology," 3rd edition, Vol. 11. John Wiley & Sons, New York, 1982.
2. Banford, W. H., and Manes, M. M., U.S. Patent 2,846,449, 1958.
3. Manly, D. G., U.S. Patent 3,021,342, 1962.
4. Garnett, D. I., and Peterson, M. L., U.S. Patent 4,172,838, 1978.
5. Farha, F. E., Jr., U.S. Patent 3,906,009, 1975.
6. Cotton, F. A., and Wilkinson, G., "Advanced Inorganic Chemistry," 3rd ed. Wiley, New York, 1972.
7. Colmenars, C. A., *Prog. Solid State Chem.* **9**, 139 (1975).
8. Grasselli, R. K., and Suresh, D. D., *J. Catal.* **25**, 273 (1972).

9. Suresh, D. D., Seely, M. J., Brazdil, J. F., and Grasselli, R. K., U.S. Patent 4,855,275, 1989.
10. Hutchings, G. J., Heneghan, C. S., Hudson, I. D., and Taylor, S. H., *Nature* **384**, 341 (1996).
11. Smith, G. M., Suzuki, H., Sonnenberger, D. C., Day, W. V., and Marks, T. J., *Organometallics* **5**, 549 (1986).
12. Madhavaram, H., Barteau, M. A., and Idriss, H., "Advanced Materials Development and Performance Proceedings" (W. G. Ferguson and W. Gao, Eds.), p. 46 (1997).
13. Madhavaram, H., and Idriss, H., *Stud. Surf. Sci. Catal.* **110**, 265 (1997).
14. Khilla, M. A., El-Fekey, S. A., and Rofail, N. H., *Radiochim. Acta* **40**, 185 (1986).
15. Madhavaram, H., Buchanan, P., and Idriss, H., *J. Vac. Sci. Technol. A* **15**, 1685 (1997).
16. Idriss, H., Kim, K. S., and Barteau, M. A., *J. Catal.* **139**, 119 (1993).
17. Ko, E. I., Benziger, J. B., and Madix, R. J., *J. Catal.* **62**, 264 (1980).
18. Madhavaram, H., and Idriss, H., *in situ* FT-IR of acetaldehyde/uranium oxides, work in progress.
19. Heinemann, C., Cornehl, H. H., and Schwartz, H., *J. Organometal. Chem.* **501**, 201 (1995).
20. Debets, P. C., *Acta Crystallogr.* **21**, 589 (1966).
21. Hoekstra, H. R., and Siegel, S., *J. Inorg. Nucl. Chem.* **18**, 154 (1961).